Early glacial maximum and deglaciation at sub-Antarctic Marion Island from cosmogenic ^{36}Cl exposure dating

Elizabeth M. Rudolph[a]*, David W. Hedding[b], Derek Fabel[c], Dominic A. Hodgson[d], Delia M. Gheorghiu[c], Richard Shanks[c] and Werner Nel[a]

[a] *Department of Geography and Environmental Science, University of Fort Hare, 1 King Williamstown Road, Alice, 5700, South Africa*

[b] *Department of Geography, University of South Africa, Florida, P O Box 392, Unisa, 0003, South Africa*

[c] *Scottish Universities Environmental Research Centre, Rankine Avenue, East Kilbride, G75 0QF, United Kingdom*

[d] *British Antarctic Survey, High Cross, Madingley Road, Cambridge, CB3 0ET, United Kingdom*

Figures: 6

Tables: 3

Abstract: 231 words

Words (main text, excluding tables, figure captions and references): 4371

*Corresponding Author:

Elizabeth M. Rudolph

Email: rudolphem@ufs.ac.za

Current Address:

Department of Geography (Building 53)

University of the Free State

205 Nelson Mandela Avenue

Park West

Bloemfontein

9300

South Africa

Abstract

Southern Hemisphere glacial chronologies can provide valuable insights into interactions between glaciation and past climate changes, but are not well constrained on most sub-Antarctic islands. We present the first cosmogenic ^{36}Cl exposure ages of deglaciated bedrock surfaces and moraine deposits from sub-Antarctic Marion Island in the southern Indian Ocean. Results show that the ice reached a local Last Glacial Maximum before 34 ka and retreated, with no re-advances, but possibly minor stand stills, until ~17 ka. This early deglaciation left island surfaces below 850 m a.s.l. ice-free after ~19 ka, and any subsequent advances during the Antarctic Cold Reversal or Holocene cooling periods would have been restricted to the interior. This glacial chronology is similar to that of some other sub-Antarctic Islands (e.g. the Kerguelen archipelago, Auckland and Campbell islands, and possibly South Georgia) and a number of other Southern Hemisphere glaciers (e.g. in Patagonia and New Zealand) and adds to evidence that suggest the Southern Hemisphere was in a glacial maxima earlier than the global LGM. We suggest a combination of declining temperatures, a northward migration of oceanic fronts and the Southern Hemisphere westerly winds (causing precipitation changes), as well as the physiography of Marion Island, created optimal conditions for glacier growth during Marine Isotope Stage (MIS) 3 instead of MIS 2. Our findings redefine the glacial history of Marion Island, and have implications for future investigations on post-glacial landscape development and ecological succession.

Keywords: Marion Island; sub-Antarctic; Cosmogenic isotopes; Chlorine-36; Last Glacial Maximum; MIS 3; Pleistocene; Geomorphology, Glacial; Glaciation; Southern Ocean

1. Introduction

Glacial oscillations of the Quaternary provide valuable opportunities to study past interactions between ice sheets and climate, offering insights into processes driving modern day climate change (Schaefer et al., 2015). Since it is increasingly apparent that the Northern- and Southern Hemispheres did not respond synchronously to past changes in climate (Clark et al., 2009; Doughty et al., 2015; Schaefer et al., 2015; De Vleeschouwer et al., 2017; Pedro et al., 2018), recent efforts have focussed on constraining the extent and timing of Southern Hemisphere glaciation, focusing on the last glacial cycle (Hodgson et al., 2014a; Bentley et al., 2014; Darvill et al., 2016). Application of radiocarbon, luminescence (OSL and IRSL) and terrestrial cosmogenic nuclide dating methods has refined Holocene and Late Pleistocene glacial chronologies for New Zealand (e.g. Putnam et al., 2013; Eaves et al., 2016; Shulmeister et al., 2019), Patagonia (e.g. Darvill et al., 2016; García et al., 2018), Tasmania (Mackintosh et al., 2006) and Antarctica (e.g. Bentley et al., 2014; Ó Cofaigh et al., 2014). On the sub-Antarctic islands, minimum ages for ice sheet retreat have been inferred by dating the onset of organic sedimentation in lakes and peat bogs with radiocarbon (e.g. Hodgson et al., 2014), or the timing of lake sediment burial with OSL and IRSL (e.g. Rainsley et al., 2019; Shulmeister et al., 2019). However, with the exception of Kerguelen (Jomelli et al., 2017; 2018) and South Georgia (Bentley et al., 2007; White et al., 2018), no chronologies have used cosmogenic isotope methods.

Sub-Antarctic Marion Island is one of the volcanic Prince Edward Islands located in the southern Indian Ocean (46°54'S, 37°45'E). Several studies have attempted to reconstruct the island's glacial history (e.g. Hall, 1980, 1981, 1982, 1983, 2004; McDougall et al., 2001; Hall et al., 2011; Hodgson et al., 2014). A scientific expedition in 1965-68 first discovered that glacial striations were restricted to the Pleistocene 'grey' lavas which led to the idea that a glacial stage must have preceded the succession of the less eroded Holocene 'black' lavas (Verwoerd, 1971). Many other glacial erosional and depositional features have subsequently been documented, supporting this initial interpretation (Hall, 1978, 1982; Nel, 2001; Hedding, 2008; Hall et al., 2011). Other geomorphological, palynological and ecological proxies have also been used to infer the island's glacial history. These include correlating stratigraphical till and geological sequences (Hall, 1978), relative-age dating of glacial and post-glacial (periglacial) geomorphic features (Sumner et al., 2002; Nel et al., 2003; Boelhouwers et al., 2008), reconstructing palaeo-temperature from snow line altitudes (Hall, 1980) and vegetation assemblages from pollen records (Scott and Hall, 1983; Scott, 1985). A link between (rapid) deglaciation and periods of volcanism has also been proposed (Hall, 1982; Kent and Grinbnitz, 1983; McDougall et al., 2001) but a reassessment of the faulting, volcanic rock, and palaeo-glacier distribution by Hall et al. (2011) suggests that this proposal is erroneous.

The most up-to-date understanding of Marion Island's late Quaternary glacial geomorphology is summarised by McDougall et al. (2001), Boelhouwers et al. (2008), Hall et al. (2011) and Hodgson et al. (2014a). In the absence of deglaciation ages, the initial hypotheses regarding the chronology and configuration of Marion Island's last glaciation proposed by Hall (1978; 1980) persist. These are that: (1) the island's local Last Glacial Maximum (lLGM) between ~11000-35000 years (~11-35 ka) ago coincided with the global Last Glacial Maximum (gLGM), in Marine oxygen Isotope Stage 2 (MIS 2) (McDougall et al., 2001). This lLGM period was defined by McDougall et al. (2001) using the time scales of Shackleton & Opdyke (1973), Bowen et al. (1986), Johnson (1982) as well as Fullerton & Richmond (1986), in order to revise the glacial reconstructions produced by Hall (1978; 1981; 1982). All glacial features within the Pleistocene grey lavas have been assigned to this last glacial stage, and Hall (1980) associates some moraines with a "cold peak" advance inferred at ~19.5 ka ago in southernmost South America (Mercer, 1976). In the absence of any alternative proposals, this timeline has been used by the broader scientific community to link maximum glaciation on Marion Island to the gLGM (e.g. Myburgh et al., 2007; Boelhouwers et al., 2008; Hall et al., 2011; Chau et al., 2019). (2) Deglaciation was rapid. It is stated by Boelhouwers et al. (2008) that retreat commenced at ~17-18 ka ago (Hall, 1978) and was near completion prior to Holocene volcanism (Hall, 1982; McDougall et al., 2001; Hall et al., 2011). (3) Significant glacial re-advances occurred during Holocene cool periods (Hall, 1978; Hall, 1980; McDougall et al., 2001; Boelhouwers et al., 2008). (4) It has also been proposed that during the lLGM, a few high-lying areas remained ice-free (Hall, 1980; Hall et al., 2011; Mortimer et al., 2011). It is assumed that these provided glacial refugia which allowed for the survival of the endemic biological communities from where they expanded across the island following deglaciation (see Schalke and Van Zinderen Bakker, 1971; Myburgh et al., 2007; Van Der Putten et al., 2010; Mortimer et al., 2012; Chau et al., 2019).

This paper constrains the timing and extent of the most recent glaciation on sub-Antarctic Marion Island through the application of cosmogenic ^{36}Cl surface exposure dating. Fourteen rock surfaces from eight sites within the island's Pleistocene grey lavas were sampled along an altitudinal transect. Four of these were from moraine boulders, eight from glacially moulded bedrock and two from a previously proposed lLGM ice-free 'nunatak'. We present the first direct ages of glacial erosional and depositional features from Marion Island, and construct a revised glacial chronology for the island's Last Glacial Maximum and deglaciation. Finally, the significance of this revised glacial chronology is discussed in context of current knowledge on the Island's landscape history and ecology, and with reference to regional climatic forcings.

2. Study Area & Methods

2.1. The setting of Marion Island

Located ±2300 km south-east of South Africa, Marion Island is the larger of the Prince Edward Islands; two oceanic shield volcanoes situated on a −200 m submarine plateau (Le Roex et al., 2012) (Figure 1). The islands are a product of an inter-plate hotspot divergence zone 370 km southeast of the Mid-Indian Ocean Plate, and comprise basalts and trachybasalts from the Atlantic suite (Verwoerd, 1971). The various lavas share a similar chemical composition (Le Roex et al., 2012). The oldest dated lava flows on Marion Island are the Pleistocene grey lavas with K-Ar ages of ~450 ka, whereas the younger black lava flows are estimated at less than 10 ka, and predominantly comprise a'a flows with some pahoehoe (McDougall et al., 2001). Although the island is accepted to be no more than 1 million years old, the surface Pleistocene grey lavas of the east coast above 410 m a.s.l. are considered equal to or younger than 50 ka (McDougall et al., 2001). Approximately 130 scoria cones scattered across the island volcano are thought to have originated throughout the Holocene (Verwoerd, 1971), though their ages have not been determined. The island has a subaerial extent of 293 km^2 (Meiklejohn and Smith, 2008), a volcanic summit just over 1240 m a.s.l. (Hedding, 2008), which is still considered active with eruptions recorded in 1980 and 2004 (Verwoerd et al., 1981; Meiklejohn and Hedding, 2005).

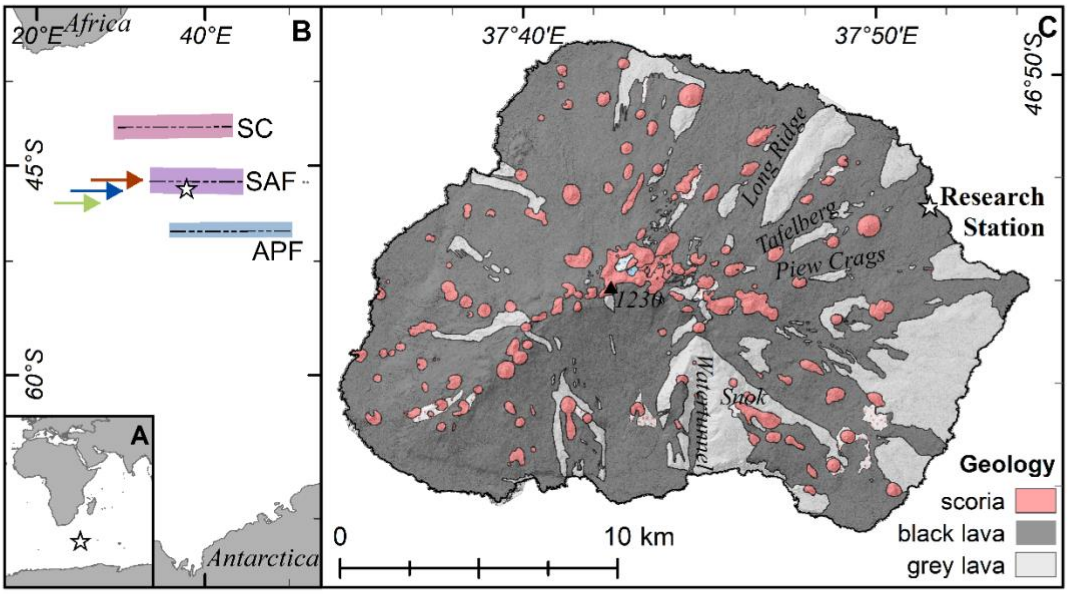

Figure 1: (A) The location of Marion Island. (B) The latitudinal range of oceanic fronts determined from point observations between 1978-1986 (dashed line indicates middle of front) (Lutjeharms & Ansorge, 2008): Subtropical Convergence (SC), Sub-Antarctic Front (SAF) and Antarctic Polar Front (APF); the theoretical position of the core of the South westerly wind track in the modern day (bottom, green arrow), in MIS 2 (top, brown) and in MIS 3 (middle, blue), adapted from Toggweiler & Russell (2008), Toggweiler (2009), Sime et al. (2013) and Shulmeister et al. (2019); (C) A simplified schematic of surface geology, adapted from Boelhouwers et al. (2008). The locations of sample sites are shown in Figure 2. Map projection: (A & B) Mercator and (C) Transverse Mercator. [size = 1.5 or 2 columns, 140 x 76 mm; colour=online only].

The island's climate is typically hyper-maritime with high but decreasing mean annual precipitation (see Hedding and Greve, 2018), currently at ~2000 mm per annum, low mean annual air temperature (~6˚C) and small seasonal and diurnal ranges (only ~4°C between winter and summer means, and <3°C daily difference) (Smith and Steenkamp, 1990). Smith and Steenkamp (1990) investigated the relationship between radiation (sunshine hours), precipitation, air- and sea surface temperatures. They only found a correlation between air and sea surface temperatures (linear correlation coefficient=0.54, $P<0.001$), emphasising the role of Southern Oceanic fronts on island temperatures, and further suggested that atmospheric circulation (passing of cyclonic fronts driven by the Southern Westerlies) modulate sunshine hours (through cloud cover), precipitation and (also) air temperature. In addition, the Subtropical Convergence, Sub-Antarctic Polar Front and the Antarctic Polar Front influence Marion Island's climate (Figure 1). Long-term observations (1978-1986) indicate strong latitudinal variation in the positions of these fronts (Lutjeharms & Ansorge, 2008).

2.2. Site selection

Sample selection for glacial geomorphological reconstructions, and especially cosmogenic dating (Dunai, 2010), requires accurate landform identification and interpretation (see Bentley et al., 2007; Hedding et al., 2018). Various glacial features are recorded within the grey lavas across the island (Hall, 1978, 1982; Nel, 2001; Hedding, 2008). On the north-east coast, sites for cosmogenic nuclide dating were selected from well-documented erosional and depositional features that lie along an altitudinal transect between Piew Crags and Long Ridge (Figures 2 and 3). These features are geomorphologically associated to the same glacial outlet or a palaeo-glacier that occupied this sector of the island (Nel, 2001; Boelhouwers et al., 2008; Hall et al., 2011). The sites include the moraine deposits on Skua Ridge, the striations on the Tafelberg complex and the glacially moulded bedrock inland from Esigangeni (formerly No Name Peak) (Hall, 1980; Nel, 2001; Boelhouwers et al., 2008; Hedding, 2008) (Figures 2, 3 and 4; and Table 1). The outcrop at Katedraalkrans was also sampled, as it has been proposed as an ice-free 'nunatak' through the lLGM (Hall et al., 2011).

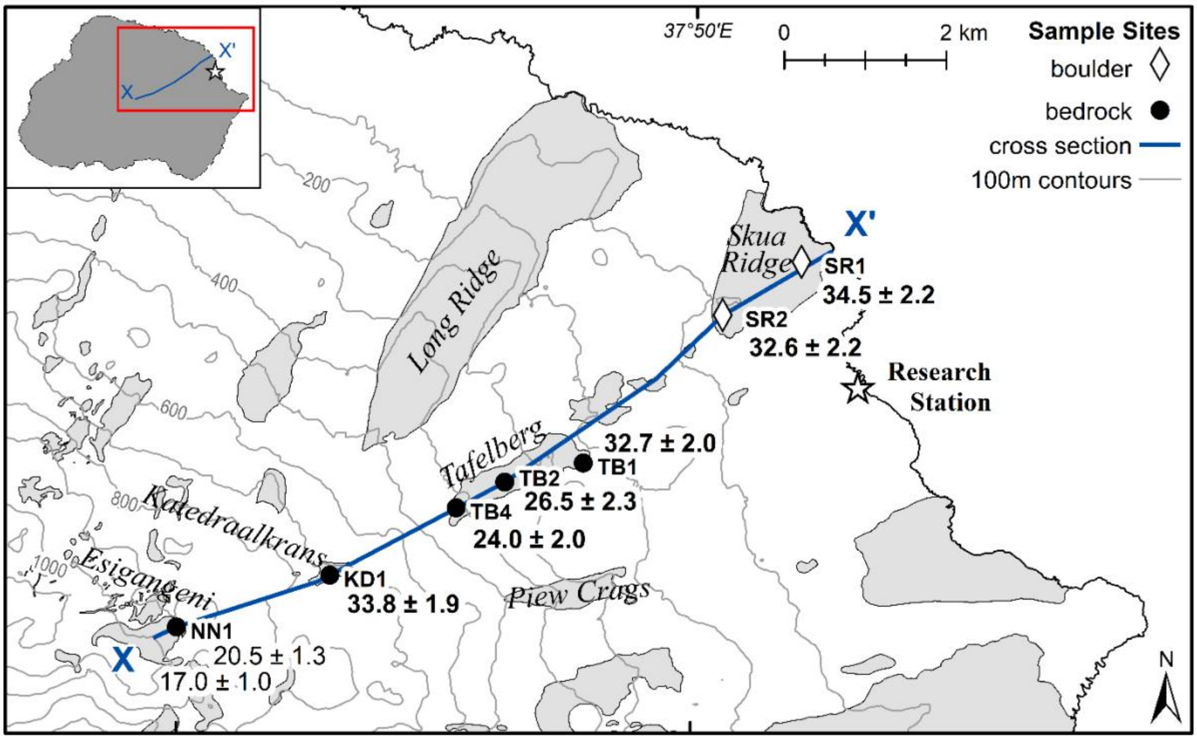

Figure 2: The location of sample sites within the Pleistocene grey lavas on Marion Island's north-east coast (see Figure 1 for island location and Table 1 for site names). The ^{36}Cl exposure ages are given in ka: normal font show individual sample ages and bold font show site ages (see Table 3). Ages are presented along a cross section (X-X') of the altitudinal transect (see Figure 5). Map projection: Transverse Mercator. [size = 2 columns, 189 x 116mm; colour=online only].

Site surveys and sampling were conducted during the SANAP Marion Island relief expeditions, in April/May 2017 and 2018. Geomorphological surveys were conducted at each site to verify previous interpretations of their glacial history. An average of one day was dedicated to sampling at each site. Sites were named alphanumerically by association with the closest landmark or glacial feature (i.e. Skua Ridge = SR; Tafelberg = TB), site number (i.e. 1, 2, 3 etc.) and sample duplicate (A-C) (Table 1). A minimum of two samples were taken per site and samples with the same site number are assumed to be closely related in age, except at Esigangeni (>900 m a.s.l.), where a difference of 9 m in altitude and 33 m horizontal distance produced a large enough error range to identify NN1A and NN1C as two different sites (Table 3).

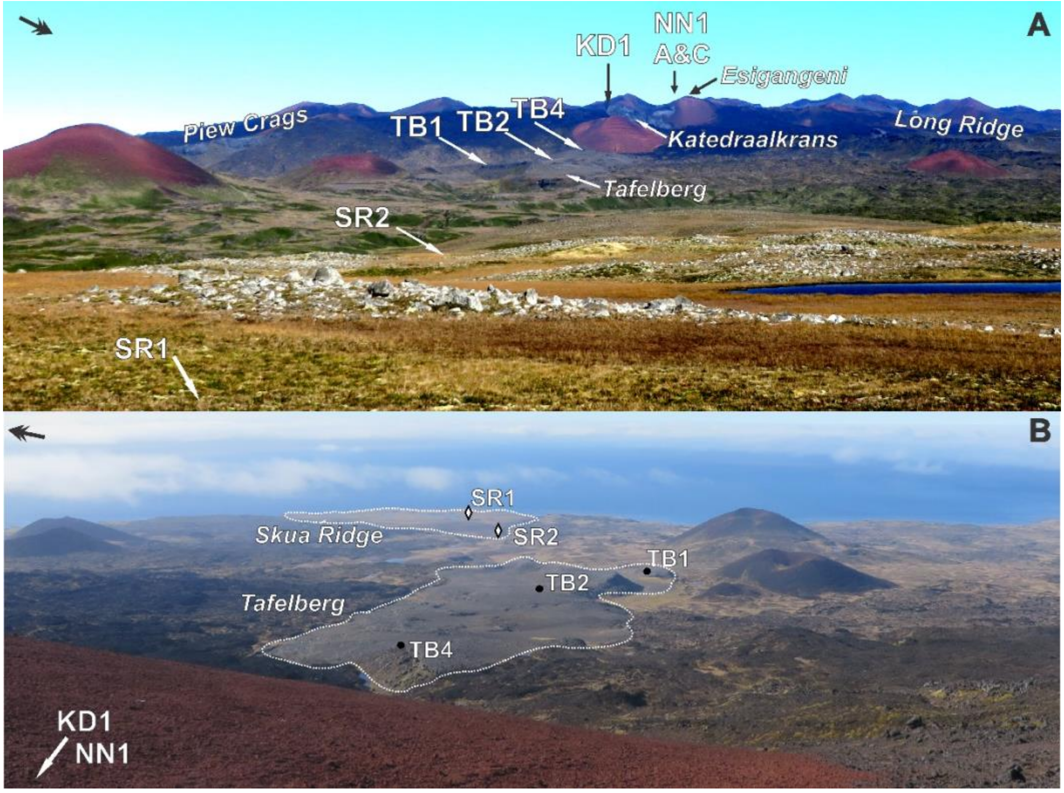

Figure 3: (A) The topographical distribution of sampling sites on the north-east coast of Marion Island taken from Skua Ridge towards the interior. (B) The location of Skua Ridge and Tafelberg, taken from inland towards the coast. Double-headed arrows indicate North. [size: 1,5-column; 140x104mm; colour=online only*]*

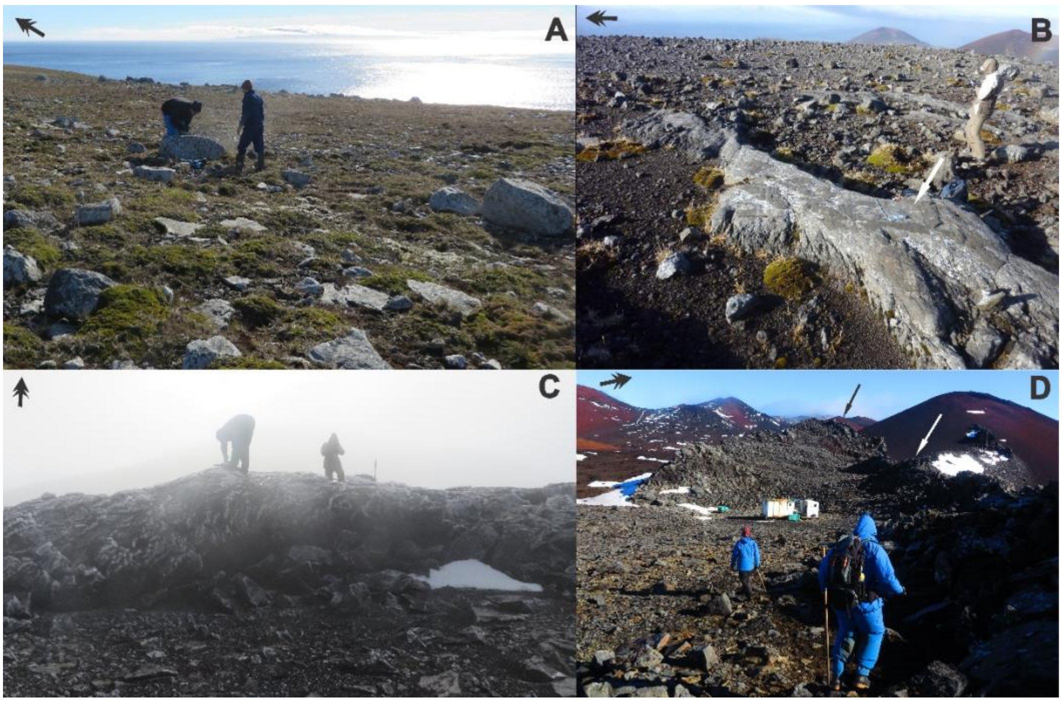

Figure 4: Examples of samples taken from (A) moraine boulders on Skua Ridge, (B) striated bedrock on Tafelberg, (C) roche moutonnées behind Esigangeni and (D) on Katedraalkrans. Double arrows indicate North. [size: 1,5-column; 140x91mm; colour=online only*]*

Table 1: Sample locations, attributes and calculated topographic shielding factors, sorted according to sample site and ascending elevation.

Sample	Lat. (D.D°)	Long. (D.D°)	Elev. (m)	Bulk dens. (g/cm3)	Thickness (cm)	Shielding Factor	Type
Skua Ridge - moraine							
SR1B	-46.86252	37.85077	84	2.62	1.8	0.997	boulder
SR1C	-46.86265	37.85078	84	2.12	1.5	0.997	boulder
SR2A	-46.86855	37.83791	96	2.79	2.2	0.999	boulder
SR2B	-46.86839	37.83853	100	2.27	2	0.994	boulder
Tafelberg - glacial pavement							
TB1A	-46.88512	37.81554	255	2.19	2.8	0.999	bedrock
TB1C	-46.88521	37.81482	256	3.14	2.5	0.976	bedrock
TB2A	-46.88732	37.80287	339	2.67	2	0.973	bedrock
TB2C	-46.88730	37.80224	341	2.13	2.2	0.999	bedrock
TB4B	-46.89027	37.79510	429	3.12	2.8	0.990	bedrock
TB4C	-46.89027	37.79510	429	2.6	2.8	0.989	bedrock
Katedraalkrans – ‘nunatak’							
KD1A	-46.89783	37.77465	759	2.64	2.12	0.999	bedrock
KD1C	-46.89857	37.77263	784	2.6	2.51	0.989	bedrock
Esigangeni – roche moutonnées							
NN1A	-46.90374	37.74988	925	2.45	2.8	0.997	bedrock
NN1C	-46.90368	37.74908	934	2.6	2.5	0.994	bedrock

2.3. Sampling

Rock samples of approximately 30x20x2 cm were extracted using a battery-operated angle grinder with diamond tipped blade, mallet and chisel. All samples were taken from surfaces with <20° dip, avoiding as far as possible erosional features such as pitting, and local shielding of bedrock by till material and erratics. Sampling locations were recorded with a handheld GPS while a digital surface model (DSM) was used to determine site elevation and calculate topographic shielding with ArcGIS according to Li (2018) (Table 1). The DSM has with a 1 x 1 m cell size resolution and vertical accuracy of 0.7 m was developed photogrammetrically using stereo Pléiades imagery. While GPS elevation values corresponded to within 10-20 m of the DSM, elevation values from the DSM were used to calculate topographic shielding. Other attribute data were collected following Dunai (2010) (Table 1).

2.4. Site description

Skua Ridge is a stable, well-vegetated, deflation moraine with undulating kettle topography which extends approximately 2 km inland from the coastal cliffs (Figures 2 and 3). Two moraine sequences have been identified on the ridge (Hall, 1978; 1980) from which two boulders were sampled at each: one on the coastal edge (SR1) and another farther inland (SR2) (Figure 4A). Both sites are located on a relatively low gradient (6-11°) and are considered to have had a low risk of sediment erosion or boulder exhumation. Boulders are highly weathered and often show dilatation fracturing, but samples were taken from boulders that were intact, showed limited signs of weathering and were embedded into the slope. Exposure ages (history) of moraine boulders are also known to be influenced by their transport history. Unaccounted inheritance or erosion could either over- or under-estimated the true exposure age of a boulder (Putkonen and Swanson, 2003; Applegate et al., 2012). For the material on Skua Ridge, rock surface erosion (through weathering) instead of inheritance is expected to have a greater influence on the precision of exposure ages.

The Tafelberg complex consists of a series of plateaus which have been glacially moulded, abraded and plucked (Figures 3 and 4B). Striated pavements and erratics are also present and the general direction of striations bears towards the coast. Three sites were sampled at Tafelberg; one at the lower (TB1), one in the middle (TB2) and one at the upper (TB4) reaches of the complex. Each site is separated by ±90 m in elevation. All samples were taken from striated surfaces of small abrasion-pluck features, except TB1A which is from a glacial pavement.

Several prominent grey lava roche moutonnées are found just inland from the scoria cone Esigangeni. The roche moutonnées have a height of ~2 m on the stoss-side and ~5 m on the plucked face and are surrounded by scoria (Figure 4C). Two adjacent roche moutonnées at the same altitude but separated by a distance of ± 30 m were sampled (NN1A & NN1C).

Katedraalkrans is a bowl-shaped grey lava outcrop with an abundance of fractured bedrock material that has been reworked by cryogenic processes to form stone-banked lobes (Nel, 2001). Though striations on bedrock have been recorded for this outcrop (Hall, 1978), they could not be found by either the current, nor earlier studies (Nel, 2001; Hedding, 2008). No other glacial evidence has been reported for this outcrop and for this reason Katedraalkrans is thought to have been a LGM ice-free nunatak. K-Ar ages for this outcrop were indeterminant (McDougall et al., 2001) and the origin of the fractured material has been ascribed to joint unloading rather than glacial unloading. Two intact bedrock surfaces were sampled along the rim of the ‘bowl’ (KD1A & KD1C) (Figure 4D).

2.5. Analysis of in situ cosmogenic ^{36}Cl

Whole rock samples were crushed and sieved to retrieve a subset of 250-710 µm for *in situ* ^{36}Cl analysis at the Scottish Universities Environmental Research Centre (SUERC). An initial ~50 g aliquot of the sample subset was etched overnight in 2 M HNO_3 and 40% HF to remove meteoric Cl and contaminants, losing ~60% of the sample during the process. Afterwards a ~5 g etched split was taken for major element analysis by ICP-OES and an additional ~12 g for accelerator mass spectrometry target preparation. The samples and two blanks were dissolved in HF with ^{35}Cl enriched spike (~ 99%). Samples were then prepared according to the methods of Marrero (2012). Chlorine was extracted and purified to produce an AgCl target for AMS analysis. Targets were pressed into a copper cathode for $^{37}Cl/^{35}Cl$ and $^{36}Cl/^{35}Cl$ ratio determination with the 5 MV accelerator mass spectrometer at SUERC. Sample geochemistry and measured ratios are presented in Tables 2 and 3. The measurement of trace elements at SUERC does not occur routinely because in past experiments inclusion of trace element data did not significant alter calculated ages. For the purpose of determining the effect of including trace elemental concentrations we recalculated the oldest and the youngest age obtained in this study using minimum and maximum concentrations for trace elements (Gale et al., 2013) and indicative U and Th values (Larsen & Gottfried, 1960). The variation in calculated ages are entirely within the calculated age uncertainties.

Exposure ages were calculated with CRONUScalc v2.0 (Marrero et al., 2016a) using the default ^{36}Cl production rates, ‘SA’ scaling (Lifton et al., 2014) and a high-energy neutron attenuation length of 160 g cm^{-2} (Marrero et al., 2016b). The respective input and output files of the calculated ^{36}Cl exposure ages, via the CRONUScalc website calculator (http://cronus.cosmogenicnuclides.rocks/2.0/html/cl/), are available online (Rudolph et al., 2019). The are no quantitative data on snow cover or erosion rates for Marion Island but these are considered negligible for the exposure age calculations.

Table 2: Chemical composition of etched whole rock, including the concentrations of the ^{36}Cl target elements Ca, K, Ti and Fe.

Sample	SiO_2 wt %	TiO_2 wt %	Al_2O_3 wt %	Fe_2O_3 wt %	MnO wt %	MgO wt %	CaO wt %	K_2O wt %	Total wt %
SR1B	64.85±1.59	4.35±0.02	9.77±0.33	10.21±0.08	0.13±0.01	1.13±0.01	7.23±0.08	1.313±0.06	98.98
SR1C	59.57±1.88	4.15±0.03	14.4±0.52	8.79±0.09	0.12±0.01	2.74±0.02	7.76±0.1	1.462±0.1	98.99
SR2A	64.66±1.84	2.93±0.02	16.08±0.56	6.17±0.05	0.1±0.01	1.54±0.01	5.57±0.08	1.964±0.11	99.01
SR2B	66.1±1.81	2.8±0.02	15.4±0.54	5.91±0.05	0.1±0.01	1.47±0.01	5.34±0.07	1.881±0.1	99.00
TB1A	53.18±1.89	6.63±0.04	10.51±0.56	16.37±0.08	0.21±0.01	3.93±0.03	6.89±0.07	1.283±0.11	99.00
TB1C	53.5±1.85	6.62±0.05	10.76±0.51	16.08±0.07	0.21±0.01	3.75±0.03	6.76±0.09	1.323±0.1	99.00
TB2A	62.41±1.92	4.37±0.03	11.78±0.53	9.81±0.1	0.15±0.01	2.91±0.03	6.12±0.11	1.454±0.1	99.00
TB2C	59.821.85	4.71±0.03	13.41±0.48	9.2±0.11	0.16±0.01	3.17±0.03	6.98±0.1	1.56±0.09	99.01
TB4B	59.31±1.91	4.46±0.02	9.4±0.53	11.07±0.09	0.17±0.01	5.11±0.04	8.49±0.12	0.989±0.1	99.00
TB4C	56.3±2.02	4.67±0.04	9.89±0.59	12.14±0.11	0.18±0.01	5.65±0.04	9.22±0.12	0.953±0.11	99.00
KD1A	57.16±1.98	5.19±0.04	11.47±0.59	11.3±0.12	0.15±0.01	4.17±0.03	8.43±0.07	1.135±0.11	99.01
KD1C	56.21±1.9	5.23±0.02	12.07±0.57	11.4±0.08	0.16±0.01	4.18±0.03	8.5±0.08	1.256±0.11	99.01
NN1A	51.46±1.92	7.52±0.03	10.81±0.53	16.14±0.11	0.22±0.01	4.03±0.04	7.65±0.1	1.167±0.1	99.00
NN1C	60.37±1.96	4.48±0.04	12.09±0.58	10.96±0.08	0.17±0.01	3.15±0.03	6.31±0.12	1.467±0.11	99.00

3. Results

The calculated cosmogenic ^{36}Cl exposure ages are provided in Table 3 and in Figures 2 and 5. The exposure ages of the boulders at Skua Ridge are consistent within 1 sigma for both SR1 and SR2. In agreement with an expected depositional sequence, the coastal moraine (SR1) produced older exposure ages than the inland sequence (SR2). The effect of erosion remains unaccounted for and these ages may be an underestimation of the true exposure age. Nevertheless, the ages of these moraine boulders conservatively suggest that the last glacial ice advance reached its maximum position prior to ~34.5 ka. No geomorphological evidence exists for subsequent ice advance over Skua Ridge. This could be due to 1) that these features simply do not exist, because as the glacier retreated (after depositing Skua Ridge) it continued to retreat until finally disappearing; or 2) glacial advances did occur (since the deposition of Skua Ridge) but evidence of these re-advances have been destroyed by subsequent post-glacial volcanism. In either case, for this sector of the island, Skua Ridge is accepted to represent the geomorphic remnants of the last ice advance to reach the current coastline. The exposure ages of the glacially moulded bedrock samples (TB1, TB2, TB4, NN1A and NN1C) indicate gradual glacial recession between ~32.7 and ~17.0 ka; with possible breaks in retreat between ~32.8-26.5 ka and 20.5-17.0 ka (Figure 5). Aside from these potential pauses, a regression analysis of exposure ages along this transect (n=12, excluding KD1), shows a significant correlation between exposure ages and altitude (r^2=0.87; P<0.001; y=-0.0184x + 34.787). From this linear regression, the lLGM ice front in this sector of the island was below present sea level before 34.5 ka ago and at ~850 m a.s.l. during the gLGM (~19 ka).

Katedraalkrans (KD1), the proposed ‘nunatak’, has an exposure age of ~33.8 ka which is ~10 ka earlier than a neighbouring, lower-lying sample (TB4; >330 m lower in altitude) and bracketed by the ages of the coastal moraines (SR1 & SR2). This indicates that the Katedraalkrans outcrop was exposed synchronous to the coastal areas at Skua Ridge, and much earlier than its immediate surrounds.

Table 3: Chlorine isotopic data with calculated ^{36}Cl exposure ages and uncertainties reported at 1σ confidence. Analytical uncertainties (in brackets) include uncertainty in the blank and counting statistics. Systematic uncertainties include uncertainty in the ^{36}Cl production rate. Site ages are calculated from sample ages with overlap at 1σ. See text for more details.

Sample[a]	**Elev. (m)**	**Mass (g)**	**Spike mass (mg)**	**^{36}Cl/Cl ($x10^{-15}$)**[b]	**Bulk Rock Cl,**[c] **(ppm)**	**^{36}Cl**[d] **(10^5 atoms/g)**	**Surface Exposure Age (ka)**	**Site Age (ka)**
Skua Ridge - moraine								
SR1B	84	12.185	1.862	72.95 ± 2.79	6.80 ± 1.77	1.91 ± 0.081	34.3 ± 2.2 (1.5)	34.5 ± 2.2
SR1C	84	12.065	1.844	79.28 ± 2.45	5.03 ± 1.69	2.06 ± 0.072	34.6 ± 2.1 (1.2)	
SR2A	96	12.413	1.848	71.99 ± 2.05	23.44 ± 2.54	2.04 ± 0.070	32.0 ± 2.0 (1.1)	32.6 ± 2.2
SR2B	100	12.308	1.857	72.11 ± 2.15	30.30 ± 2.89	2.15 ± 0.077	33.1 ± 2.3 (1.2)	
Tafelberg - glacial pavement								
TB1A	255	12.324	1.822	76.59 ± 2.51	14.97 ± 2.12	2.05 ± 0.076	31.3 ± 1.9 (1.2)	32.7 ± 2.0
TB1C	256	12.095	1.822	85.73 ± 2.57	15.17 ± 2.16	2.35 ± 0.081	34.0 ± 2.0 (1.2)	
TB2A	339	12.392	1.833	74.19 ± 2.07	66.06 ± 4.59	2.63 ± 0.097	27.2 ± 2.4 (1.0)	26.5 ± 2.3
TB2C	341	12.568	1.875	73.89 ± 2.15	67.77 ± 4.68	2.66 ± 0.100	25.8 ± 2.1 (1.0)	
TB4B	429	12.099	1.885	76.32 ± 2.35	50.71 ± 3.92	2.61 ± 0.099	24.0 ± 2.0 (0.9)	24.5 ± 2.0
TB4C	429	12.376	1.853	80.77 ± 2.46	43.41 ± 3.51	2.58 ± 0.096	24.9 ± 1.9 (0.9)	
Katedraalkrans – 'nunatak'								
KD1A	759	12.104	1.896	126.08 ± 3.73	6.53 ± 1.8	3.48 ± 0.113	33.1 ± 1.9 (1.1)	33.8 ± 1.9
KD1C	784	12.456	1.88	129.78 ± 3.7	7.05 ± 1.77	3.47 ± 0.110	34.4 ± 1.9 (1.1)	
Esigangeni – roche moutonnées								
NN1A	925	12.019	1.831	96.17 ± 2.92	24.69 ± 2.63	2.83 ± 0.099	20.5 ± 1.3 (0.7)	20.5 ± 1.3
NN1C	934	12.04	1.823	90.74 ± 2.7	2.86 ± 1.57	2.32 ± 0.076	17.0 ± 1.0 (0.6)	17.0 ± 1.0

[a] AMS targets were prepared and measured at SUERC.

[b] Normalised to standard Z93-0005 produced at Prime Lab (Purdue University) with a nominal ^{36}Cl/Cl ratio of 1.2E-12.

[c] Stable Cl concentrations were calculated by AMS isotope dilution (Di Nicola et al., 2009). All samples were spiked with non-natural Cl with a ^{35}Cl/^{37}Cl ratio of 21.52 ± 0.02 atoms/atom.

[d] Procedural blank ^{36}Cl/Cl = 3.46 ± 0.48 $x10^{-15}$. Blank corrections for ^{36}Cl concentrations ranged from between 1.5 and 5%.

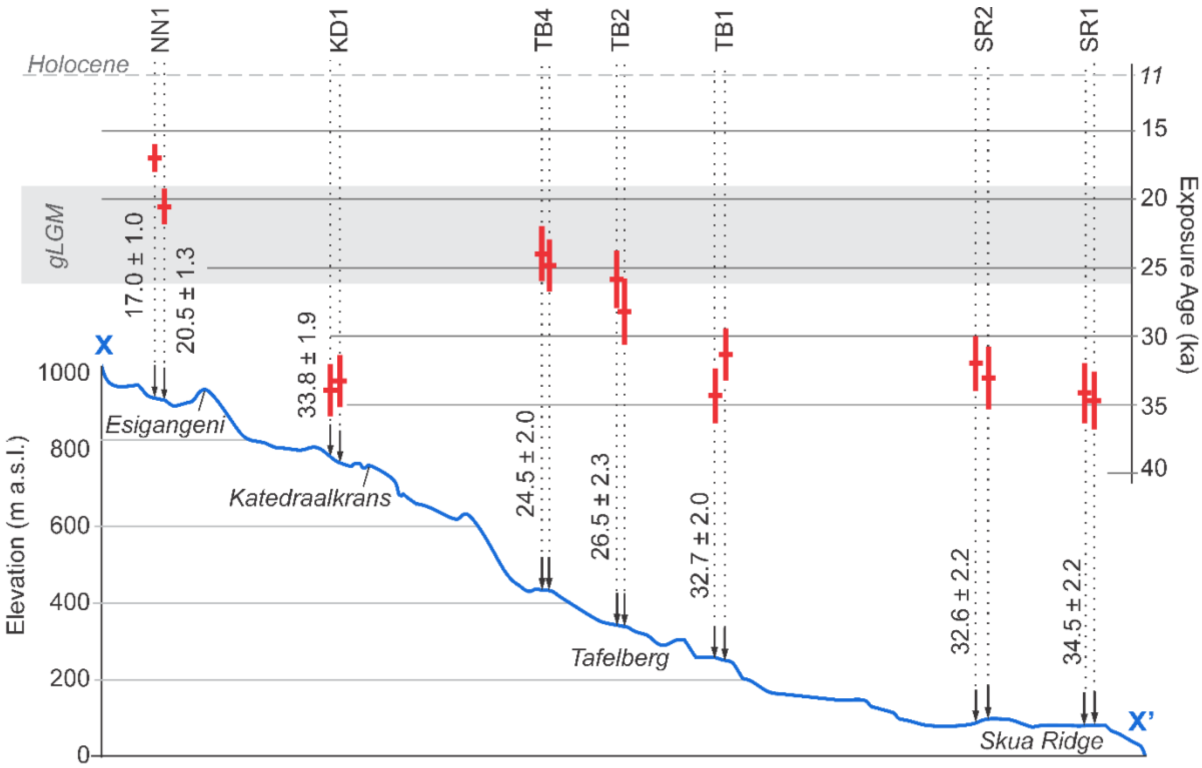

Figure 5: A cross section (X-X') showing sample locations and exposure ages along an altitudinal transect from Skua Ridge across Tafelberg to the interior (see Figure 2). Exposure ages and systematic uncertainties (see Table 3) are shown for individual samples (red ┼) and per site (inverted text). The gLGM period (Clark et al., 2009) is provided for reference. See text for details. [size=1.5 columns; 190x124mm; colour=online only]

4. Discussion

4.1. An early lLGM and deglaciation on Marion Island

The cosmogenic ^{36}Cl exposure ages of glacial landforms presented here require a revision of the glacial chronology of Marion Island. The evidence for an lLGM before 34 ka, pre-dates previous studies that have attributed the formation of glacial landforms on Marion Island to the gLGM (Hall, 1978, 1980, 1982; Nel, 2001; Hall, 2004; Boelhouwers et al., 2008; Hedding, 2008; Hall et al., 2011), MIS 2 (McDougall et al. 2001), or a 'cold peak' at 19.5 ka (Hall, 1980).

Instead, our results indicate a maximum ice extent sometime before 34.5 ka, with ice receding until at least 17.0 ka, with no chronological or geomorphological evidence for substantial re-advances during this period. This left the island largely ice-free, except for an ice cap above 900 m a.s.l. whose remnants can still be seen today (Sumner et al., 2004). Since the island's lLGM likely occurred in a currently off-shore position (Hodgson et al., 2014a), the exact timing and full spatial extent of the lLGM will remain unresolved until high resolution bathymetry data are acquired.

Previous hypotheses of a rapid deglaciation (post-LGM; Hall, 1982) are also refuted since the exposure ages along the altitudinal sequence show slow deglaciation from the coastal moraine (~34.5 ka) to the highest bedrock (~17.0 ka). This represents a ~17 ka retreat over ~9 km horizontal distance. However, there could have been periods of minor ice stand stills, occurring within the retreat rate decreases between 32.7-26.5 and 20.5-17.0 ka ago, the latter possibly a signal of the gLGM peak (~19 ka ago). Given that there is no evidence for cosmogenic inheritance, the ages of the bedrock surfaces indicate continuous deglaciation and suggest that any post-gLGM advances (e.g. during the Antarctic Cold Reversal or Little Ice Age) would have been restricted to the interior. It has been proposed that these late Glacial and Holocene glacial advances might have resulted in the small lateral moraines in Watertunnel Valley (~120 m a.s.l), and a terminal moraine associated with the cirque basin at Snok (~470 m a.s.l.) (Boelhouwers et al., 2008) (see Figure 1). The current data set does not provide evidence for Holocene glaciation, therefore, the age of these features as well as the “[fresh] striations on basalts” in the interior (Hall et al., 2011), requires further investigation.

The proposal that Katedraalkrans was an ice-free nunatak, and biological refuge, through the last glacial (Hall et al., 2011, Van Der Putten et al., 2010; Mortimer et al., 2011; 2012; Chau et al., 2019) also needs to be revised. Whilst Katedraalkrans was ice-free during the gLGM, and exposed much earlier than its immediate surrounds (~10 ka earlier), it was most likely glaciated before 33.8 ka, synchronous with the lLGM beyond Skua Ridge prior to 34.5 ka. This means that additional biological refugia must have been present elsewhere on Marion Island during the lLGM to allow the persistence of the island’s endemic species. Our results suggest that low lying areas between the main outlet glaciers and a more extensive coastal zone (now inundated by rising post glacial sea levels) are the most likely candidates.

For Marion Island, the documented rates of periglacial processes (Sumner et al., 2002; Nel et al., 2003; Boelhouwers et al., 2008), soil development (Haussmann et al., 2010), peat growth (Van Der Putten et al., 2010), and ecological succession and colonization (Mortimer et al., 2012; Chau et al., 2019) as well as the age and sequence of 'Holocene' volcanism (McDougall et al., 2001; Verwoerd 1971) should also be reviewed. Our current understanding of these processes are largely based on the premise that the island was under full glacial conditions during the gLGM and had undergone rapid deglaciation prior to the Holocene. The rates of these aforementioned processes may, therefore, be over-estimated given the earlier lLGM and slower deglaciation.

4.2. Comparison to other Southern Hemisphere glacial chronologies

The early lLGM at Marion Island adds to evidence of extensive MIS 3 glacial maxima in the sub-Antarctic and elsewhere in the Southern Hemisphere (Figure 6). Many of these MIS 3 maxima were more extensive than the later MIS 2 ice limits. There are similarities with other sub-Antarctic islands, such as Kerguelen where the maximum ice extent (dated on land) was reached before ~41 ka (Jomelli et al., 2018), and possibly South Georgia where the maximum has not yet been dated (Graham et al., 2017). An early maximum has also been proposed for Auckland and Campbell islands between 62-72 ka based on a flow line model (Rainsley et al., 2019). Today, glaciers persist on Kerguelen and South Georgia (Graham et al., 2017; Jomelli et al., 2018) but have completely disappeared from Auckland and Campbell Islands before ~15 ka ago (Rainsley et al., 2019). The retreat sequence on Marion Island is in broad agreement with the patterns suggested for these sub-Antarctic islands, though any MIS 2 ice advances would have been restricted to the inland ice cap.

Selected mountain glaciers in New Zealand (e.g. Tongariro Massif and Cobb Valley) and Tasmania (e.g. on Mt. Field) also show a similar recessional pattern to the sub-Antarctic Islands (Figure 6). Millennia of slow retreat or glacial stand still followed a MIS 3 maxima (which varied between 34-57 ka ago) and subsequent, less extensive, advances occurred during the gLGM (Mackintosh et al., 2006; Eaves et al., 2016; 2019).

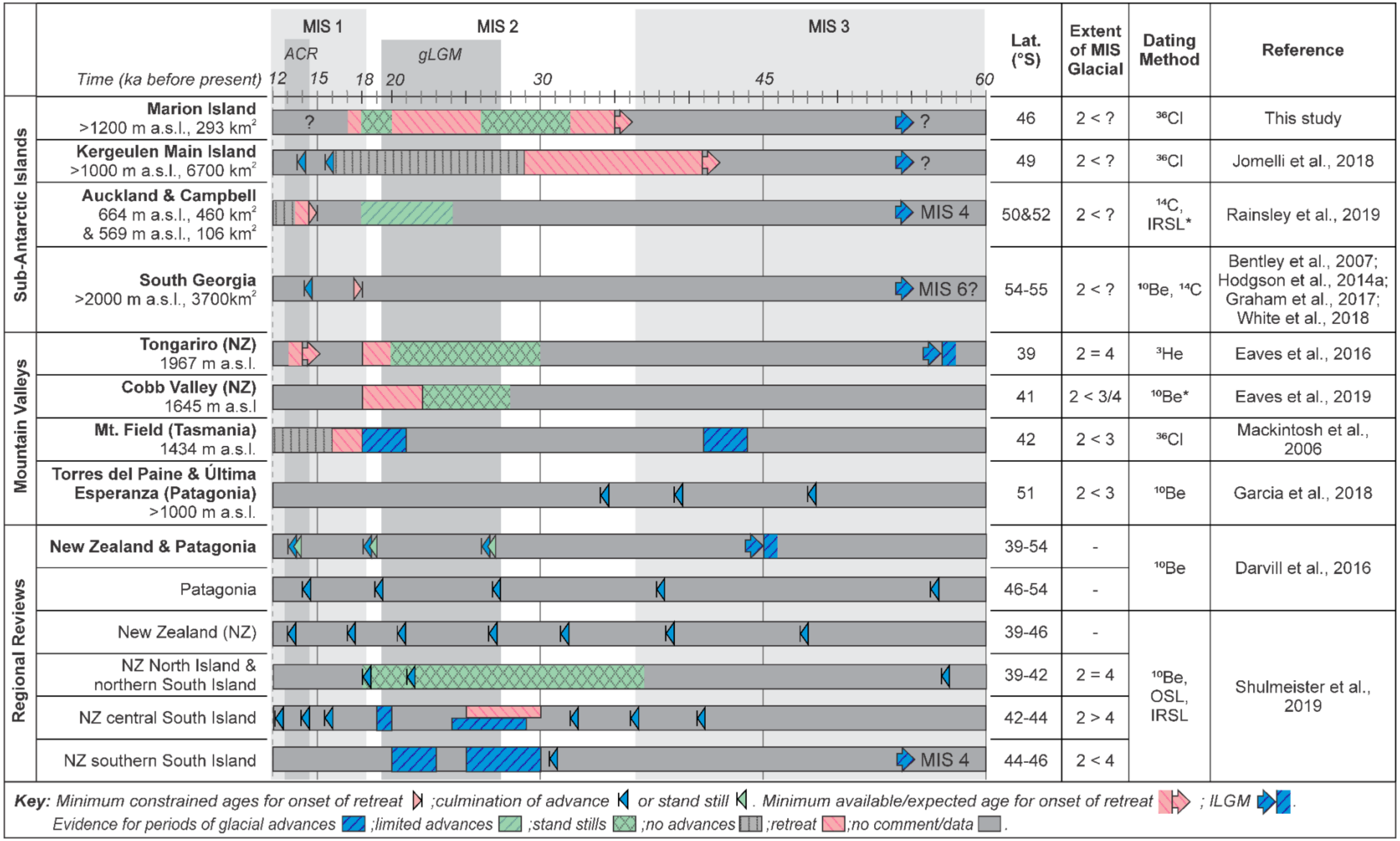
MIS 1
MIS 2
MIS 3
ACR
gLGM
Time (ka before present)
12
15
18
20
30
45
60
Lat. (°S)
Extent of MIS Glacial
Dating Method
Reference
Sub-Antarctic Islands
Marion Island >1200 m a.s.l., 293 km²
?
?
46
2 < ?
³⁶Cl
This study
Kergeulen Main Island >1000 m a.s.l., 6700 km²
?
49
2 < ?
³⁶Cl
Jomelli et al., 2018
Auckland & Campbell 664 m a.s.l., 460 km² & 569 m a.s.l., 106 km²
MIS 4
50&52
2 < ?
¹⁴C, IRSL*
Rainsley et al., 2019
South Georgia >2000 m a.s.l., 3700km²
MIS 6?
54-55
2 < ?
¹⁰Be, ¹⁴C
Bentley et al., 2007; Hodgson et al., 2014a; Graham et al., 2017; White et al., 2018
Mountain Valleys
Tongariro (NZ) 1967 m a.s.l.
39
2 = 4
³He
Eaves et al., 2016
Cobb Valley (NZ) 1645 m a.s.l
41
2 < 3/4
¹⁰Be*
Eaves et al., 2019
Mt. Field (Tasmania) 1434 m a.s.l.
42
2 < 3
³⁶Cl
Mackintosh et al., 2006
Torres del Paine & Última Esperanza (Patagonia) >1000 m a.s.l.
51
2 < 3
¹⁰Be
Garcia et al., 2018
Regional Reviews
New Zealand & Patagonia
39-54
-
¹⁰Be
Darvill et al., 2016
Patagonia
46-54
-
New Zealand (NZ)
39-46
-
NZ North Island & northern South Island
39-42
2 = 4
¹⁰Be, OSL, IRSL
Shulmeister et al., 2019
NZ central South Island
42-44
2 > 4
NZ southern South Island
MIS 4
44-46
2 < 4
Key: Minimum constrained ages for onset of retreat ;culmination of advance or stand still . Minimum available/expected age for onset of retreat ; ILGM .
Evidence for periods of glacial advances ;limited advances ;stand stills ;no advances ;retreat ;no comment/data .

Figure 6: A comparison of glacial chronologies between selected islands and mountain valleys in the Southern Hemisphere. Regional reviews provide standardised summaries of previous published chronologies. The chronostratigraphic units are from Railsback et al., 2015 (MIS), Clark et al., 2009 (gLGM) and Putnam et al., 2010 (ACR). Glaciation events were determined by geomorphological dating (radiocarbon, cosmogenic nuclides, OSL, IRSL) or modelling and are indicated by colour (see figure key). Summit peaks/headwall elevation and current surface extent are given. The comparative extent of MIS glacial events are indicated as provided by authors. Other details are discussed in text. [size: 2-coloumn, landscape; 260x155mm; colour=online only*].*

Regional summaries of Patagonia and New Zealand show broadly synchronous glacial chronologies which also indicate MIS 3 or earlier glacial maxima (Darvill et al., 2016; Shulmeister et al., 2019) (Figure 6). However, contrary to the sub-Antarctic islands these ice sheets also advanced in MIS 2 and, in New Zealand, during the gLGM to positions equal to (e.g. North Island and northern South Island) or more extensive (e.g. central South Island) than the MIS3 ice limits (Shulmeister et al., 2019). However, not all glaciers followed the same pattern (e.g. Cobb Valley; Eaves et al., 2019).

4.3. Causes of an earlier (MIS 3) lLGM

Drivers of Southern Hemisphere climate change have been described by Schaefer et al. (2015), Darvill et al. (2016), Rainsley et al. (2019) and Shulmeister et al. (2019). These include astronomical forcings (summer insolation minima, seasonality) (e.g. Vandergoes et al., 2005; De Vleeschouwer et al., 2017), the Southern Ocean (sea ice extent, ocean circulation, bipolar 'seesaw' and stratification, sea surface temperatures, CO_2 sequestration) (e.g. Crosta et al., 2004; Benz et al., 2016; Pedro et al., 2018) and the atmosphere (air temperatures, frontal systems, Southern Westerly Winds) (e.g. Toggweiler, 2009; Ó Cofaigh et al., 2014; Sime et al., 2016). Identifying the contribution of these drivers to the MIS 3 glacial advances is not straightforward (Shulmeister et al., 2019). For example, in New Zealand, a minimum summer insolation at ~31.5 ka is used to account for the ~32 ka glaciation (Vandergoes et al., 2005), but it does not provide a suitable explanation for earlier MIS 3 advances (e.g. ~38-45 ka; Shulmeister et al., 2019). Even though insolation minima can influence glacial advances in some regions, they are not considered an important driver of glacial maxima in the Southern Hemisphere between 18-45 ka (Doughty et al., 2015). Instead, a combination of drivers, including the position of ocean fronts and the Southern Hemisphere westerly winds were involved (Putnam et al., 2013; Darvill et al., 2016; Rainsley et al., 2019; Shulmeister et al., 2019).

The Southern Hemisphere westerlies migrate latitudinally in response to changes in atmospheric temperature gradients: being farther north during colder conditions, and southwards under warming conditions (Toggweiler, 2009). In addition, the migration of the westerly wind belt is also associated with changes in Southern Ocean circulation and sea surface temperatures (Toggweiler & Russell, 2008) and, in the absence of topography and rain shadow effects, with rainfall (Garreaud et al., 2009). Considering these factors, the continued downward temperature trend seen in Antarctic ice core records during MIS 3 (EPICA, 2006) is consistent with an expansion of Southern Ocean sea ice and the northward migration of ocean fronts and the Southern Hemisphere westerly winds (Crosta et al., 2004; Putnam et al., 2013; Darvill et al., 2016; Shulmeister et al., 2019). Under these conditions, a northward shift of the southern westerly wind belt would progressively bring more precipitation to the Southern Hemisphere islands and continental landmasses with decreasing latitude. Shulmeister et al. (2019) uses this hypothesis to account for the differences in timing of glacial maxima at different latitudes in New Zealand: at 44.4°S by 32 ka ago (MIS 3) and 42.6°S by 25 ka ago (MIS 2). This hypothesis may also explain why mid-latitude (sub-Antarctic) islands, like Marion, experienced a more extensive glaciation during MIS 3, and limited or no advances during MIS 2. In this scenario, an increase in precipitation (as snow) coincided with the passing of the westerly wind track over Marion Island during the MIS 3 glacial advance, whereas continued northward migration of the westerly winds starved the glaciers of moisture during MIS2 (see Figure 1). This is consistent with the overall decrease in precipitation simulated for the Indian sector of the Southern Ocean under gLGM maximum sea ice conditions (Sime et al., 2013, 2016). By the end of MIS 2 / gLGM (~18 ka ago), rising temperatures would have forced the westerlies to migrate back southwards (Toggweiler, 2009). This time, however, warmer temperatures would more likely have brought rain instead of snow to Marion Island, and therefore did not halt the deglaciation.

Local topography can also explain some of the differences in Southern Hemisphere glacier behavior. Larger and higher altitude islands (e.g. South Georgia, Kerguelen) and mountain ranges (e.g. Andes and Southern Alps) have larger (interconnected) glacial basins, compared with smaller islands (e.g. Marion and Auckland islands) and isolated valleys (e.g. Cobb Valley and Mt. Field). The larger / higher altitude islands could therefore sustain glaciers and ice caps through the changes in moisture supply brought about by migrations of the westerly wind belt through MIS 3 and 2 (Figure 6), and then re-advance during the gLGM and ACR (e.g. Kerguelen or New Zealand's central South Island).

The results from this study emphasise the role of the Southern Hemisphere westerly winds and local topography in determining the timing and extent of Southern Hemisphere glacial maxima (e.g. Shulmeister et al., 2019) in MIS 3 rather than MIS2.

5. Conclusions

This paper presents the first cosmogenic ^{36}Cl surface exposure ages of fourteen rock surfaces from eight sites along an altitudinal transect on the north-eastern coast of Marion Island. The results refute some long-standing assumptions about the timing of the Island's most recent glacial maximum. First, based on exposure ages of glacial deposits within the low altitude Pleistocene grey lavas, Marion Island's lLGM occurred prior to ~34 ka and did not coincide with the gLGM. Second, instead of a rapid pre-Holocene deglaciation, glacial retreat on Marion Island was slow, possibly with minor stand stills, and continued without re-advancing until ~17 ka when much of the island was ice free. Third, Holocene ice advances appear to have been confined to the island's interior above 900 m a.s.l. with ice cover at ~19 ka ago probably extending no lower than 850 m a.s.l. These results require a re-evaluation of the location and timing of the ice-free areas which acted as biological refugia during the last glaciation, and a reconsideration of the rates of periglacial processes, soil and peat formation, and ecological succession. Further investigation is needed to confirm when the ice reached its maximum extent (offshore) in MIS 3, and to establish whether there is evidence of glacial response(s) in the interior of Marion Island such as the Snok and Watertunnel sites during Late Pleistocene or Holocene cooling events (e.g. MIS 2, Antarctic Cold Reversal or Little Ice Age). Fourth, the new retreat sequence for Marion Island is similar to that seen on the Kerguelen archipelago

(Jomelli et al., 2018), and some mountain valleys in New Zealand (Eaves et al., 2016; 2019) and Australia (Mackintosh et al., 2006). This supports the hypothesis that the position of the Southern Hemisphere westerly winds and differences in topography were key drivers of MIS3 glacial maxima.

Future work on Marion Island will focus on cosmogenic nuclide dating of glacial features on the southern and western coasts and in the interior above 900 m a.s.l. This will contribute to wider syntheses of Southern Hemisphere glacial chronologies (e.g. Hodgson et al., 2014a), and more comprehensive reconstructions of climate-glacier interactions.

Acknowledgements

The South African National Antarctic Programme and the Department of Environmental Affairs for logistical support, and the National Research Foundation for financial support (SANAP-NRF: 110723). We are grateful for the endurance of our field assistants, the expertise of the staff at SUERC, and the use of the facilities at the Departments of Geography and Geology at the University of the Free State. Lastly, we are grateful for the reviewers…

Data Availability

Datasets related to the article can be found at [https://data.mendeley.com/datasets/xx7znfc8xv/draft/b?a=MTQ3YWE5NzMtZTc3My00Y2I5LThjY2MtYzQ3MmJjMzMxYjcx], an open source online data repository hosted at Mendeley Data (Rudolph et al., 2019).

References

Applegate, P.J., Urban, N.M., Keller, K., Lowell, T.V, Laabs, B.J.C., Kelly, M.A., Alley, R.B. 2012. Improved moraine age interpretations through explicit matching of geomorphic process models to cosmogenic nuclide measurements from single landforms. Quaternary Research, 77(2), 293–304. https://doi.org/10.1016/j.yqres.2011.12.002

Bentley, M.J., Evans, D.J.A., Fogwill, C.J., Hansom, J.D., Sugden, D E., Kubik, P.W. 2007. Glacial geomorphology and chronology of deglaciation, South Georgia, sub-Antarctic. Quaternary Science Reviews, 26(5–6), 644–677. https://doi.org/10.1016/j.quascirev.2006.11.019

Bentley, M.J., Ó Cofaigh, C., Anderson, J.B., Conway, H., Davies, B., Graham, A.G.C., … Zwartz, D. 2014. A community-based geological reconstruction of Antarctic Ice Sheet deglaciation since the Last Glacial Maximum. Quaternary Science Reviews, 100, 1–9. https://doi.org/10.1016/j.quascirev.2014.06.025

Benz, V., Esper, O., Gersonde, R., Lamy, F., Tiedemann, R. 2016. Last Glacial Maximum sea surface temperature and sea-ice extent in the Pacific sector of the Southern Ocean. Quaternary Science Reviews, 146, 216–237. https://doi.org/10.1016/j.quascirev.2016.06.006

Boelhouwers, J.C., Meiklejohn, K.I., Holness, S., Hedding, D.W. 2008. Geology, geomorphology and climate change. In Chown, S.L., Froneman, P.W. (Eds.), Prince Edward Islands: land-sea interactions (pp. 65–96). Stellenbosch: SUN PReSS. http://hdl.handle.net/10019.1/101907

Bowen, D.Q., Richmond, G.M., Fullerton, D.S., Šibrava, V., Fulton, R.J., Velichko, A.A. 1986. Correlation of Quaternary glaciations in the northern hemisphere. Quaternary Science Reviews, 5, 509–510. https://doi.org/10.1016/0277-3791(86)90218-0

Chau, J.H., Born, C., McGeoch, M.A., Bergstrom, D., Shaw, J., Terauds, A., Mairal, M., Le Roux, J.J., Jansen van Vuuren, B. 2019. The influence of landscape, climate, and history on spatial genetic patterns in keystone plants (Azorella) on sub-Antarctic islands. Molecular Ecology, 28, 3291–3305. https://doi.org/10.1111/mec.15147

Clark, P.U., Dyke, A.S., Shakun, J.D., Carlson, A.E., Clark, J., Wohlfarth, B., Mitrovica, J.X. Hostetler, S.W., McCabe, A.M. 2009. The Last Glacial Maximum. Science, 325(5941), 710–714. https://doi.org/10.1126/science.1172873

Crosta, X., Sturm, A., Armand, L., Pichon, J.J. 2004. Late Quaternary sea ice history in the Indian sector of the Southern Ocean as recorded by diatom assemblages. Marine Micropaleontology, 50(3–4), 209–223. https://doi.org/10.1016/S0377-8398(03)00072-0

Darvill, C.M., Bentley, M.J., Stokes, C.R., Shulmeister, J. 2016. The timing and cause of glacial advances in the southern mid-latitudes during the last glacial cycle based on a synthesis of exposure ages from Patagonia and New Zealand. Quaternary Science Reviews, 149, 200–214. https://doi.org/10.1016/j.quascirev.2016.07.024

De Vleeschouwer, D., Vahlenkamp, M., Crucifix, M. Pälike, H. 2017. Alternating Southern and Northern Hemisphere climate response to astronomical forcing during the past 35 m.y., Geology, 45(4), 375–378. https://doi.org/10.1130/G38663.1

Di Nicola, L., Schnabel, C., Wilcken, K.M., & Gméling, K. 2009. Determination of chlorine concentrations in whole rock: Comparison between prompt-gamma activation and isotope-dilution AMS analysis. Quaternary Geochronology, 4(6), 501–507. https://doi.org/10.1016/j.quageo.2009.08.001

Doughty, A.M., Schaefer, J.M., Putnam, A.E., Denton, G.H., Kaplan, M.R., Barrell, D.J.A., Andersen, B.G., Kelley, S.E., Finkel, R.C., Schwartz, R. 2015. Mismatch of glacier extent and summer insolation in Southern Hemisphere mid-latitudes. Geology, 43(5), 407–410. https://doi.org/10.1130/G36477.1

Dunai, T. 2010. Cosmogenic Nuclides: Principles, concepts and applications in earth surface sciences. New York: Cambridge University Press. https://doi.org/10.1007/s13398-014-0173-7.2

Eaves, S.R., Mackintosh, A.N., Anderson, B.M. 2019. Climate amelioration during the Last Glacial Maximum recorded by a sensitive mountain glacier in New Zealand. Geology, 47(4), 299–302. https://doi.org/10.1130/G45543.1

Eaves, S.R., Mackintosh, A.N., Winckler, G., Schaefer, J M., Alloway, B.V, Townsend, D. B. 2016. A cosmogenic 3He chronology of late Quaternary glacier fluctuations in North Island, New Zealand (39°S). Quaternary Science Reviews, 132, 40–56. https://doi.org/10.1016/j.quascirev.2015.11.004

EPICA members. 2006. One-to-one coupling of glacial climate variability in Greenland and Antarctica. Nature, 444(7116), 195–198. https://doi.org/10.1038/nature05301

Fullerton, D.S., Richmond, G.M. 1986. Comparison of the marine oxygen isotope record, the eustatic sea level record, and the chronology of glaciation in the United States of

America, Quaternary Science Reviews, 5, 197–200. https://doi.org/10.1016/0277-3791(86)90185-X

Gale A., C. A. Dalton, C. H. Langmuir, Y. Su, and J.-G. Schilling (2013), The mean composition of ocean ridge basalts,Geochem. Geophys. Geosyst., 14, 489–518,García, J.L., Hein, A.S., Binnie, S.A., Gómez, G.A., González, M.A., Dunai, T.J. 2018. The MIS 3 maximum of the Torres del Paine and Última Esperanza ice lobes in Patagonia and the pacing of southern mountain glaciation. Quaternary Science Reviews, 185, 9–26. https://doi.org/10.1016/j.quascirev.2018.01.013

Garreaud, R.D., Vuille, M., Compagnucci, R., Marengo, J. 2009. Present-day South American climate. Palaeogeography, Palaeoclimatology, Palaeoecology, 281(3–4), 180–195. https://doi.org/10.1016/j.palaeo.2007.10.032

Graham, A.G.C.C., Kuhn, G., Meisel, O., Hillenbrand, C.-D., Hodgson, D.A., Ehrmann, W., Wacker, L., Wintersteller, P., Dos Santos Ferreira, C., Römer, M., White, D., Bohrmann, G. 2017. Major advance of South Georgia glaciers during the Antarctic Cold Reversal following extensive sub-Antarctic glaciation. Nature Communications, 8, 14798. https://doi.org/10.1038/ncomms14798

Hall, K. 1978. Quaternary glacial geology of Marion Island. PhD Thesis, University of the Orange Free State: Bloemfontein, pp 369.

Hall, K. 1980. Late glacial ice cover and palaeotemperatures on sub-Antarctic Marion Island. Palaeogeography, Palaeoclimatology, Palaeoecology, 29, 243–259. https://doi.org/10.1016/0031-0182(79)90084-1

Hall, K. 1981. Quantitative analysis of till lithology on Marion Island, South African Journal of Science, 77, 86–90.

Hall, K. 1982. Rapid deglaciation as an initiator of volcanic activity: an hypothesis. Earth Surface Processes and Landforms, 7, 45–51. https://doi.org/10.1017/CBO9781107415324.004

Hall, K. 1983. A reconstruction of the Quaternary ice cover on Marion Island. In Oliver, R. James, P. & Jago, J. (Eds.), Antarctic Earth Science (pp. 461–464). Canberra: Australian Academy of Science.

Hall, K. 2004. Quaternary glaciation of the sub-Antarctic Islands. In Ehlers, J. & Gibbard, P. (Eds.), Quaternary Glaciations-extent and chronology (Part III, pp. 339–345). Amsterdam: Elsevier.

Hall, K., Meiklejohn, K.I., Bumby, A. 2011. Marion Island volcanism and glaciation. Antarctic Science, 23(02), 155–163. https://doi.org/10.1017/S0954102010000878

Haussmann, N., Aldahan, A., Boelhouwers, J., Possnert, G. 2010. ^{10}Be application to soil development on Marion Island, southern Indian Ocean. Nuclear Instruments and Methods in Physics Research, Section B: Beam Interactions with Materials and Atoms, 268(7–8), 1058–1061. https://doi.org/10.1016/j.nimb.2009.10.097

Hedding, D.W. 2008. Spatial inventory of landforms in the recently exposed central highland of Sub-Antarctic Marion Island. South African Geographical Journal, 90(1), 11–21. https://doi.org/10.1080/03736245.2008.9725307

Hedding, D.W., Brook, M.S., Winkler, S. 2018. Old landscape, new eyes: revisiting geomorphological research in the Southern Alps of New Zealand. New Zealand Geographer, 74(2), 109–112. https://doi.org/10.1111/nzg.12189

Hedding, D.W., Greve, M. 2018. Decreases in precipitation on sub-Antarctic Marion Island: implications for ecological and geomorphological processes, Weather, 73(6), 203. https://doi.org/10.1002/wea.3245

Hodgson, D.A., Graham, A.G.C., Roberts, S.J., Bentley, M.J., Ó Cofaigh, C., Verleyen, E., … Smith, J.A. 2014a. Terrestrial and submarine evidence for the extent and timing of the Last Glacial Maximum and the onset of deglaciation on the maritime- Antarctic and sub-Antarctic islands. Quaternary Science Reviews, 100, 137–158. https://doi.org/10.1016/j.quascirev.2013.12.001

Hodgson, D.A., Graham, A.G.C., Griffiths, H.J., Roberts, S.J., Ó Cofaigh, C., Bentley, M.J., & Evans, D.J.A. 2014b. Glacial history of sub-Antarctic South Georgia based on the submarine geomorphology of its fjords. Quaternary Science Reviews, 89, 129–147. https://doi.org/10.1016/j.quascirev.2013.12.005

Hughes, P.D., Gibbard, P.L., Ehlers, J. 2013. Timing of glaciation during the last glacial cycle: Evaluating the concept of a global "Last Glacial Maximum" (LGM). Earth-Science Reviews, 125, 171–198. https://doi.org/10.1016/j.earscirev.2013.07.003

Hughes, P.D., Gibbard, P.L. 2015. A stratigraphical basis for the Last Glacial Maximum (LGM). Quaternary International, 383, 174–185. https://doi.org/10.1016/j.quaint.2014.06.006

Johnson, R.G. 1982. Brunhes-Matuyama Magnetic Reversal Dated at 790,000 yr B.P. by Marine-Astronomical Correlations, Quaternary Research. 2017/01/20. Cambridge University Press, 17(2), pp. 135–147. https://doi.org/10.1016/0033-5894(82)90055-2

Jomelli, V., Mokadem, F., Schimmelpfennig, I., Chapron, E., Rinterknecht, V.,… Keddadouche, K. 2017. Sub-Antarctic glacier extensions in the Kerguelen Region (49°S, Indian Ocean) over the past 24,000 years constrained by ^{36}Cl moraine dating. Quaternary Science Reviews, 162, 128–44. https://doi.org/10.1016/j.quascirev.2017.03.010

Jomelli, V., Schimmelpfennig, I., Favier, V., Mokadem, F., Landais, A., Rinterknecht, V., … Keddadouche, K. 2018. Glacier extent in sub-Antarctic Kerguelen archipelago from MIS 3 period: Evidence from ^{36}Cl dating. Quaternary Science Reviews, 183, 110–123. https://doi.org/10.1016/j.quascirev.2018.01.008

Kent, L., Grinbnitz, K.H. 1983. Problematic Quaternary successions on Marion Island: volcanogenic or glaciogenic. South African Journal of Antarctic Research, 13, 15–23.

Larsen, E.S. & Gottfried, D. 1960. Uranium and thorium in selected suites of igneous rocks. American Journal of Science, Bradley Vol., Vol 258-A, 1960, P.151-169.

Le Roex, A.P., Chevallier, L., Verwoerd, W.J., Barends, R. 2012. Petrology and geochemistry of Marion and Prince Edward Islands, Southern Ocean: Magma chamber processes and source region characteristics. Journal of Volcanology and Geothermal Research, 223-224, 11–28. https://doi.org/10.1016/j.jvolgeores.2012.01.009

Li, Y.K. 2018. Determining topographic shielding from digital elevation models for cosmogenic nuclide analysis: a GIS model for discrete sample sites. Journal of Mountain Science, 15(5), 939–947. https://doi.org/10.1007/s11629-018-4895-4

Lutjeharms, J., Ansorge, I. J. 2008. Oceanographic setting of the Prince Edward Islands. In Chown, S. L. & Froneman, P. W. (Eds.), Prince Edward Islands: land-sea interactions in a changing ecosystem (pp. 17–38). Stellenbosch: SUN PReSS. http://hdl.handle.net/10019.1/101907

Lifton, N., Sato, T., Dunai, T.J., 2014. Scaling in situ cosmogenic nuclide production rates using analytical approximations to atmospheric cosmic-ray fluxes. Earth Planetary Science Letters, 386, 149-160. https://doi.org/10.1016/j.epsl.2013.10.052

Mackintosh, A.N., Barrows, T.T., Colhoun, E.A., Fifield, L.K. 2006. Exposure dating and glacial reconstruction at Mt. Field, Tasmania, Australia, identifies MIS 3 and MIS 2 glacial advances and climatic variability. Journal of Quaternary Science, 21(4), 363–376. https://doi.org/10.1002/jqs.989

Marrero, S.M., 2012. Calibration of Cosmogenic Chlorine-36. Dissertation. New Mexico Institute of Mining and Technology, USA. http://www.ees.nmt.edu/outside/alumni/papers/2012d_marrero_s.pdf

Marrero, S.M., Phillips, F.M., Borchers, B., Lifton, N., Aumer, R., Balco, G. 2016a. Cosmogenic nuclide systematics and the CRONUScalc program. Quaternary Geochronology, 31, 160–187. https://doi.org/10.1016/j.quageo.2015.09.005

Marrero, S.M., Phillips, F.M., Caffee, M.W., Gosse, J.C. 2016b. CRONUS-Earth cosmogenic 36Cl calibration. Quaternary Geochronology, 31, 199–219. https://doi.org/10.1016/j.quageo.2015.10.002

McDougall, I., Verwoerd, W.J., Chevallier, L. 2001. K–Ar geochronology of Marion Island, Southern Ocean. Geological Magazine, 138(1), 1–17. https://doi.org/10.1017/S0016756801005039

Meiklejohn, K.I., Hedding, D.W. 2005. Report on Marion Island (South Africa). In R. Wunderman (Ed.), Bulletin of the Global Volcanism Network (30:2). Smithsonian Institution. https://doi.org/https://doi.org/10.5479/si.GVP.BGVN200502-234070

Meiklejohn, K.I., Smith, V.R. 2008. Surface areas of altitudinal zones on sub-Antarctic Marion Island. Polar Biology, 31(2), 259–261. https://doi.org/10.1007/s00300-007-0389-5

Mercer, J. 1976. Glacial history of southernmost South America, Quaternary Research, 6, 125–166.

Mortimer, E., Jansen van Vuuren, B., Lee, J.E., Marshall, D.J., Convey, P., Chown, S.L. 2011. Mite dispersal among the southern ocean islands and antarctica before the last glacial maximum. Proceedings of the Royal Society B: Biological Sciences, 278(1709), 1247–1255. https://doi.org/10.1098/rspb.2010.1779

Mortimer, E., Jansen van Vuuren, B., Meiklejohn, K.I., Chown, S.L. 2012. Phylogeography of a mite, Halozetes fulvus, reflects the landscape history of a young volcanic island in the sub-Antarctic. Biological Journal of the Linnean Society, 105, 131–145. https://doi.org/10.1111/j.1095-8312.2011.01770.x

Myburgh, M., Chown, S.L., Daniels, S.R., Van Vuuren, B.J. 2007. Population structure, propagule pressure, and conservation biogeography in the sub-Antarctic: Lessons from indigenous and invasive springtails: Biodiversity research. Diversity and Distributions, 13(2), 143–154. https://doi.org/10.1111/j.1472-4642.2007.00319.x

Nel, W., Holness, S., Meiklejohn, K.I. 2003. Observations on rapid mass movement and screes on Sub-Antarctic Marion Island. South African Journal of Science, 99(3–4), 177–181.

Nel, W. 2001. A spatial inventory of glacial, periglacial and rapid mass movement forms on part of Marion Island: Implications for Quaternary environmental change. MSc Thesis, University of Pretoria: Pretoria, pp. 73.

Ó Cofaigh, C., Davies, B.J., Livingstone, S.J., Smith, J.A., Johnson, J.S., Hocking, E.P., … Simms, A.R. 2014. Reconstruction of ice-sheet changes in the Antarctic Peninsula since the Last Glacial Maximum. Quaternary Science Reviews, 100, 87–110. https://doi.org/10.1016/j.quascirev.2014.06.023

Pedro, J.B., Jochum, M., Buizert, C., He, F., Barker, S., Rasmussen, S.O. 2018. Beyond the bipolar seesaw: Toward a process understanding of interhemispheric coupling.

Quaternary Science Reviews, 192, 27–46. https://doi.org/10.1016/j.quascirev.2018.05.005

Putkonen, J., Swanson, T. 2003. Accuracy of cosmogenic ages for moraines. Quaternary Research, 59(2), 255–261. https://doi.org/10.1016/S0033-5894(03)00006-1

Putnam, A.E., Denton, G.H., Schaefer, J.M., Barrell, D.J.A., Andersen, B.G., Finkel, R.C., Schwartz, R., Doughty, A.M., Kaplan, M.R., Schlüchter, C. 2010. Glacier advance in southern middle-latitudes during the Antarctic Cold Reversal. Nature Geoscience, 3(10), 700–704. https://doi.org/10.1038/ngeo962

Putnam, A.E., Schaefer, J M., Denton, G.H., Barrell, D.J.A., Birkel, S.D., Andersen, B.G., Kaplan, M.R. Finkel, R.C., Schwartz, R., Doughty, A.M. 2013. The Last Glacial Maximum at 44°S documented by a 10Be moraine chronology at Lake Ohau, Southern Alps of New Zealand. Quaternary Science Reviews, 62, 114–141. https://doi.org/10.1016/j.quascirev.2012.10.034

Railsback, L.B., Gibbard, P.L., Head, M.J., Voarintsoa, N.R.G., Toucanne, S. 2015. An optimized scheme of lettered marine isotope substages for the last 1.0 million years, and the climatostratigraphic nature of isotope stages and substages. Quaternary Science Reviews, 111, 94–106. https://doi.org/10.1016/j.quascirev.2015.01.01 2

Rainsley, E., Turney, C.S.M., Golledge, N.R., Wilmshurst, J.M., McGlone, M.S., Hogg, A.G., Li, B., Thomas, Z.A., Roberts, R., Jones, R.T., Palmer, J.G., Flett, V., De Wet, G., Hutchinson, D.K., Lipson, M.J., Fenwick, P., Hines, B., Binetti, U., Fogwill, C.J. 2019. Pleistocene glacial history of the New Zealand subantarctic islands. Climate of the Past, 15(2), 423–448. https://doi.org/10.5194/cp-15-423-2019

[dataset] Rudolph, E.M, Hedding, D.W., Fabel, D., Hodgson, D.A., Gheorghiu, D.M., Shanks, R., Nel, W. 2019. The first cosmogenic 36Cl exposure ages for glacial features on sub-Antarctic Marion Island: raw CRONUScalc inputs & outputs. Mendeley Data, V1, https://data.mendeley.com/datasets/xx7znfc8xv/draft/b?a=MTQ3YWE5NzMtZTc3My00Y2I5LThjY2MtYzQ3MmJjMzMxYjcx

Schaefer, J.M., Putnam, A.E., Denton, G.H., Kaplan, M.R., Birkel, S., Doughty, A.M., … Schluechter, C. 2015. The Southern Glacial Maximum 65,000 years ago and its Unfinished Termination. Quaternary Science Reviews, 114, 52–60. https://doi.org/10.1016/j.quascirev.2015.02.009

Schalke, H.J.W.G., van Zinderen Bakker, E.M. 1971. History of the vegetation. In Van Zinderen Bakker, E.M. Winterbottom, J.M., Dyer, R.A. (Eds.), Marion and Prince Edward Islands (pp. 89–97). Cape Town: Balkema.

Scott, L. 1985. Palynological Indications of the Quaternary Vegetation History of Marion Island (Sub-Antarctic). Journal of Biogeography, 12(5), 413–431. https://doi.org/10.2307/2844951

Scott, L., Hall, K. 1983. Palynological evidence for interglacial vegetation cover on Marion Island, Subantarctic. Palaeogeography, Palaeoclimatology, Palaeoecology, 41, 35–43. https://doi.org/10.1016/0031-0182(83)90074-3

Shackleton, N.J., Opdyke, N.D. 1973. Oxygen isotope and palaeomagnetic stratigraphy of Equatorial Pacific Core V28-238: Oxygen isotope temperatures and ice volumes on a 105 year and 106 year scale. Quaternary Research, 3(1), 39–55. https://doi.org/10.1016/0033-5894(73)90052-5

Shulmeister, J., Thackray, G.D., Rittenour, T.M., Fink, D., Patton, N.R. 2019. The timing and nature of the last glacial cycle in New Zealand. Quaternary Science Reviews, 206, 1–20. https://doi.org/10.1016/J.QUASCIREV.2018.12.020

Sime, L.C., Hodgson, D., Bracegirdle, T.J., Allen, C., Perren, B., Roberts, S., De Boer, A.M. 2016. Sea ice led to poleward-shifted winds at the Last Glacial Maximum: The influence of state dependency on CMIP5 and PMIP3 models. Climate of the Past, 12(12), 2241–2253. https://doi.org/10.5194/cp-12-2241-2016

Sime, L. C., Kohfeld, K. E., Le Quéré, C., Wolff, E. W., de Boer, A. M., Graham, R. M., Bopp, L. 2013. Southern Hemisphere westerly wind changes during the Last Glacial Maximum: model-data comparison. *Quaternary Science Reviews*, *64*, 104–120. https://doi.org/10.1016/j.quascirev.2012.12.008

Smith, V.R., & Steenkamp, M. 1990. Climatic change and its ecological implications at a subantarctic island. Oecologia, 85, 14–24.

Sumner, P.D., Meiklejohn, K.I., Boelhouwers, J.C., Hedding, D.W. 2004. Climate change melts Marion Island's snow and ice. South African Journal of Science, 100(7–8), 395–398.

Sumner, P.D., Nel, W., Holness, S., Boelhouwers, J.C. 2002. Rock weathering characteristics as relative-age indicators for glacial and post-glacial landforms on Marion Island. South African Geographical Journal, 84(2), 153–157. https://doi.org/10.1080/03736245.2002.9713766

Toggweiler, J.R. 2009. Shifting Westerlies. Science, 323(5920), 1434–1435. https://doi.org/10.1126/science.1169338

Toggweiler, J.R., Russell, J. 2008. Ocean circulation in a warming climate. Nature, 451(7176), 286–288. https://doi.org/10.1038/nature06590

Van Der Putten, N., Verbruggen, C., Ochyra, R., Verleyen, E., Frenot, Y. 2010. Subantarctic flowering plants: Pre-glacial survivors or post-glacial immigrants? Journal of Biogeography, 37(3), 582–592. https://doi.org/10.1111/j.1365-2699.2009.02217.x

Vandergoes, M. J., Newnham, R. M., Preusser, F., Hendy, C. H., Lowell, T. V, Fitzsimons, S. J., Hogg, A.G., Kasper, H.U., Schlüchter, C. 2005. Regional insolation forcing of late Quaternary climate change in the Southern Hemisphere. Nature, 436(7048), 242–245. https://doi.org/10.1038/nature03826

Verwoerd, W.J. 1971. Geology. In Van Zinderen Bakker, E.M. Winterbottom, J.M., Dyer, R.A. (Eds.), Marion and Prince Edward Islands: report on the South African biological and geological research expedition 1965-1966 (pp. 40–62). Cape Town: A.A. Balkema.

Verwoerd, W.J., Russell, S., Berruti, A. 1981. 1980 volcanic eruption reported on Marion Island. Earth and Planetary Science Letters, 54(1), 153–156. https://doi.org/10.1016/0012-821X(81)90076-5

White, D.A., Bennike, O., Melles, M., Berg, S., Binnie, S.A. 2018. Was South Georgia covered by an ice cap during the Last Glacial Maximum? In Siegert, M., Jamieson, S., White, D.A. (Eds.), Exploration of Subsurface Antarctica: Uncovering Past Changes and Modern Processes, 461, (pp. 49–59). London: Geological Society, Special Publications. https://doi.org/10.1144/SP461.4